

Fig.S1. The release behavior of IR820 from PHSM@IC NPs in the simulative physiological condition.

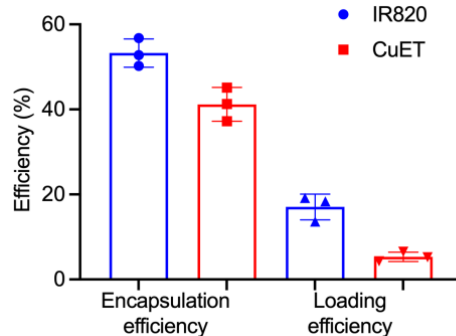


Fig.S2. The encapsulation and loading efficiency of IR820 and CuET

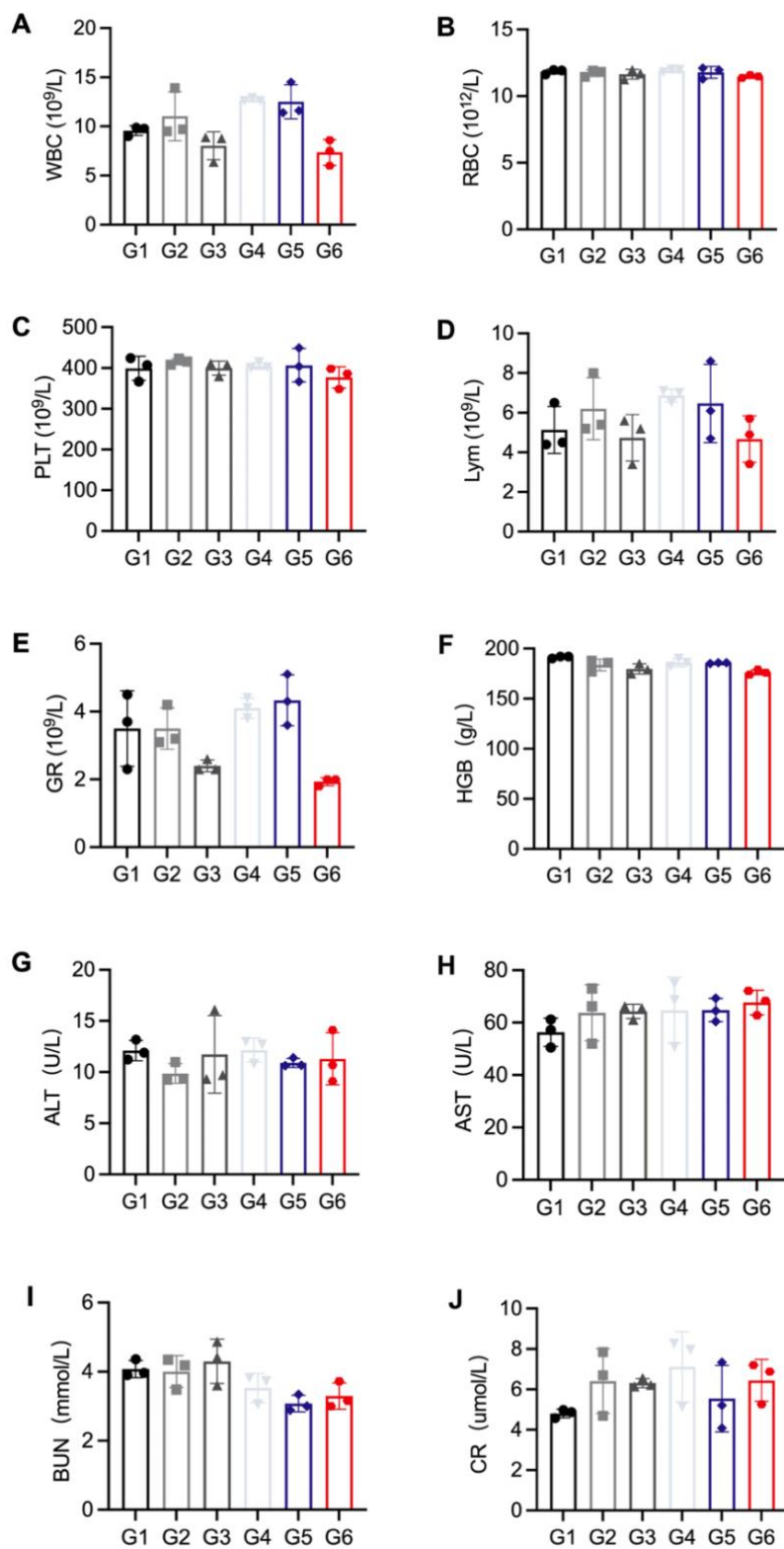


Fig. S3. Blood routine and liver and kidney function of mice with different treatment groups.

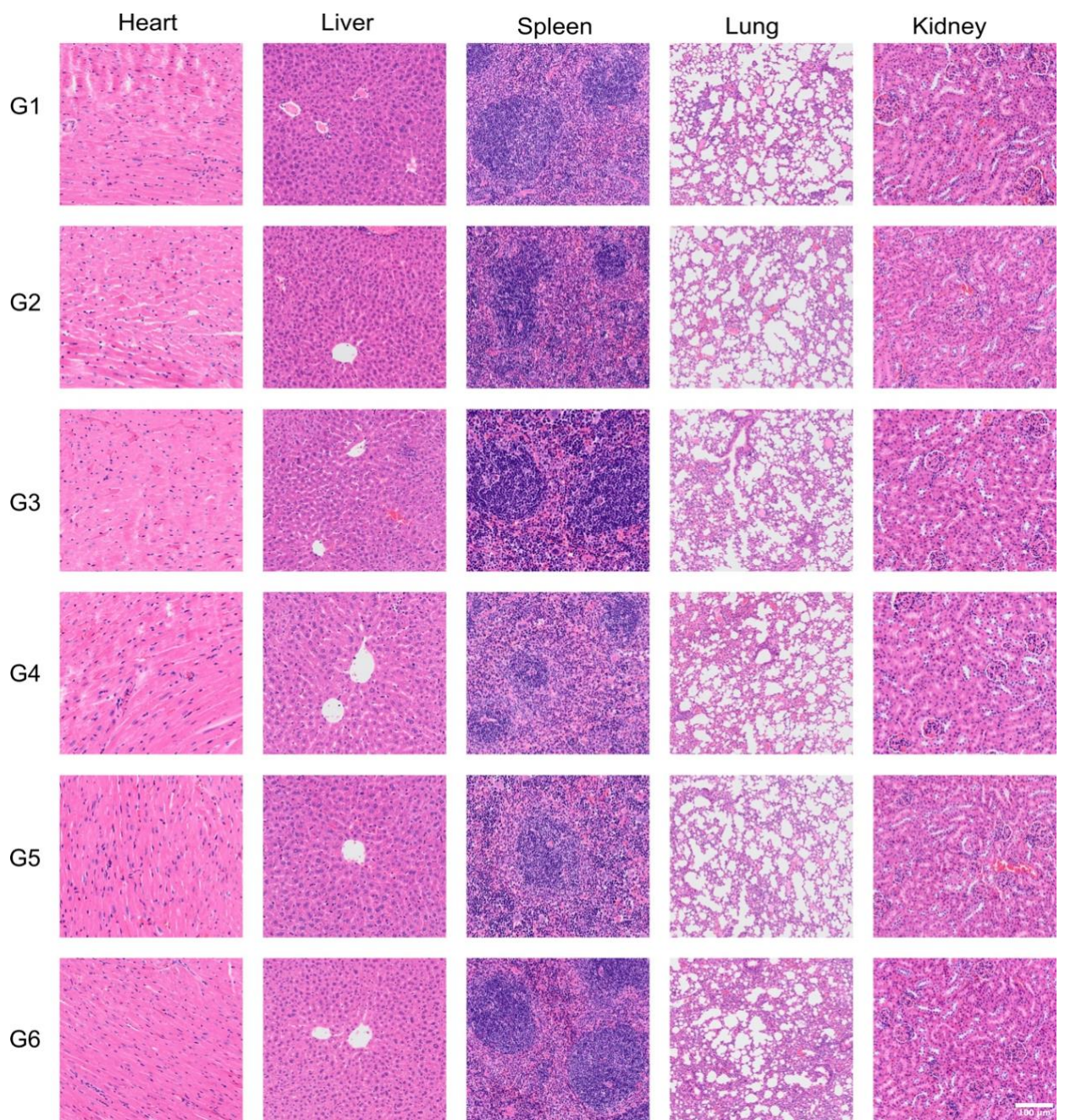


Fig. S4. The assessment of main organs by H&E staining.

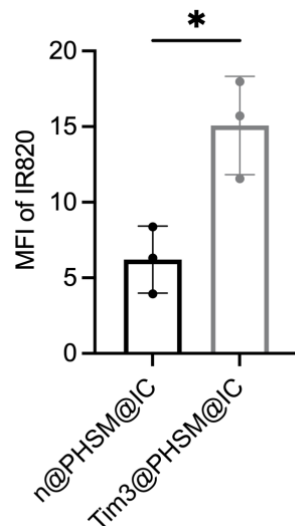


Fig. S5. Semi-quantification of IR820 in Mb49 cells treated with n@PHSM@IC and Tim3@PHSM@IC NPs. Data are represented as mean  $\pm$  SD. Student t-test was performed, \* $p$  < 0.05, n=3.

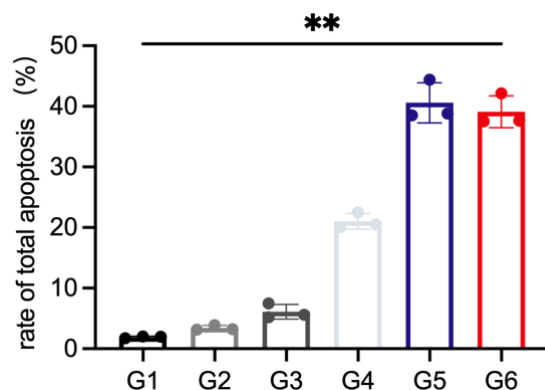


Fig. S6. Semi-quantification of apoptosis rate in Mb49 cells with various treatments via FCM. Data are represented as mean  $\pm$  SD. p values were calculated via one-way ANOVA test with Tukey correction. \* $p$  < 0.05, \*\* $p$  < 0.01, n=3.

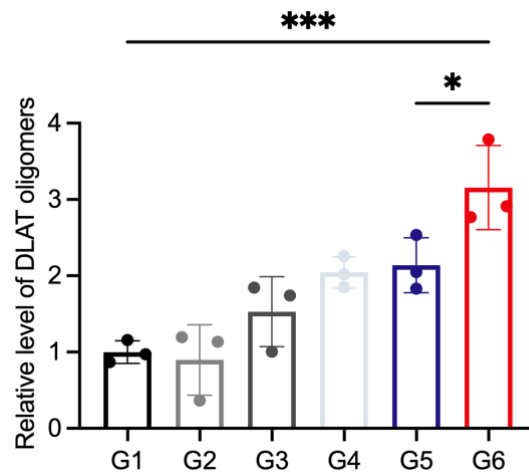


Fig. S7. Semi-quantification of DLAT oligomers expression by western blot. Data are represented as mean  $\pm$  SD. p values were calculated via one-way ANOVA test with Tukey correction. \*p < 0.05, \*\*p < 0.01, \*\*\*p < 0.001, n=3.

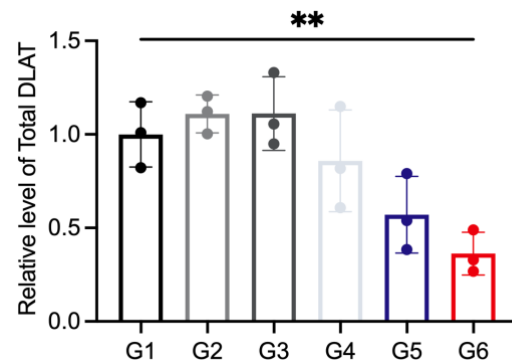


Fig. S8. Semi-quantification of total DLAT expression by western blot. Data are represented as mean  $\pm$  SD. p values were calculated via one-way ANOVA test with Tukey correction. \*p < 0.05, \*\*p < 0.01, n=3.

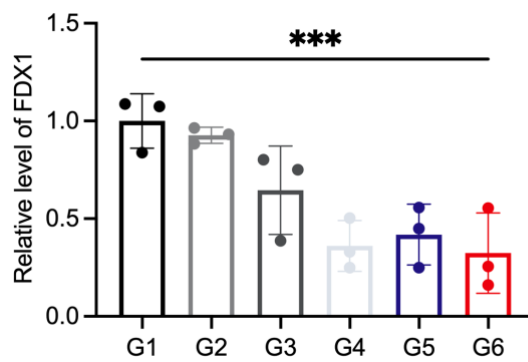


Fig. S9. Semi-quantification of FDX1 expression by western blot. Data are represented as mean  $\pm$  SD. p values were calculated via one-way ANOVA test with Tukey correction. \*p < 0.05, \*\*p < 0.01, \*\*\*p < 0.001, n=3.

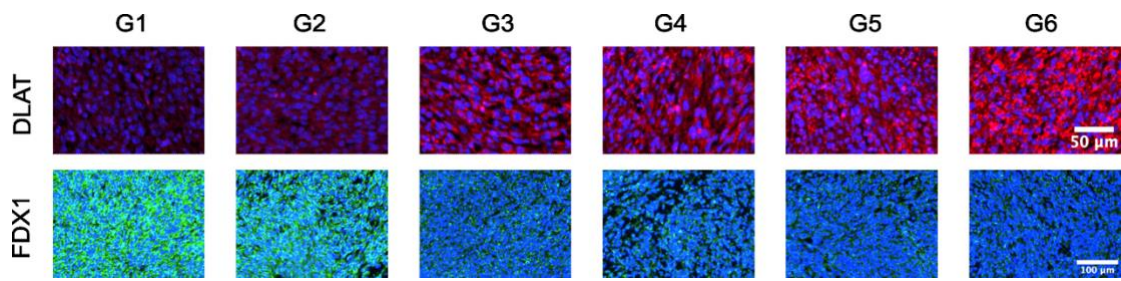


Fig. S10. DLAT and FDX1 immunofluorescence images of tumor tissues from mice in different treatment groups.

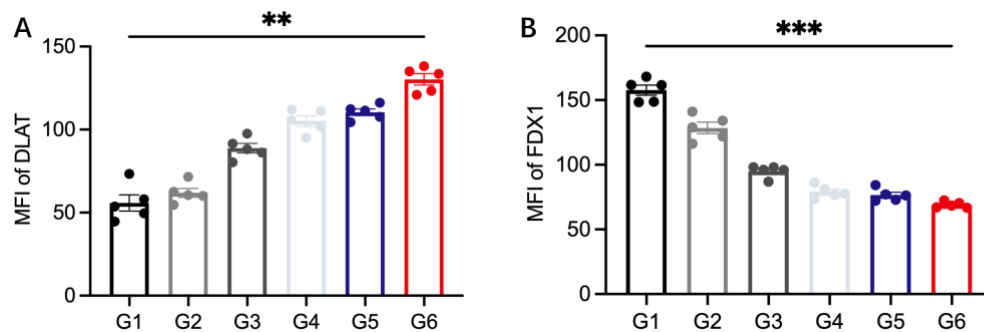


Fig. S11. Semi-quantification of DLAT (A) and FDX1 (B) immunofluorescence images of tumor tissues from mice in different treatment groups. Data are represented as mean  $\pm$  SEM. p values were calculated via one-way ANOVA test with Tukey correction. \*p < 0.05, \*\*p < 0.01, \*\*\*p < 0.001, n=3.



Fig. S12. CD47 content on biomimetic nanoparticles by western blot, n=3.

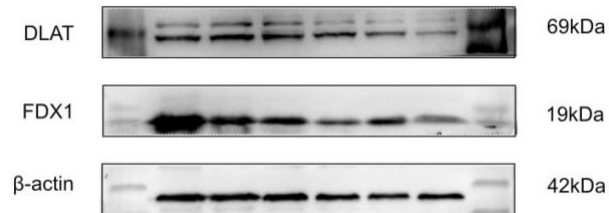


Fig. S13. In vivo total DLAT and FDX1 expression by western blot, n=3.

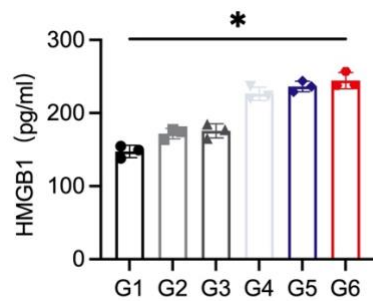


Fig. S14. HMGB1 release in MB49 cell supernatants from various treatment groups, Data are represented as mean  $\pm$  SD. p values were calculated via one-way ANOVA test with Tukey correction. \*p < 0.05, n=3.

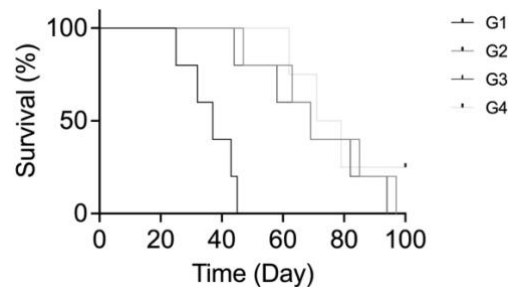


Fig. S15. Survival curves of tumor-bearing mice in different groups within 100 days. Kaplan-Meier curve was used for survival curve analysis, n=5.

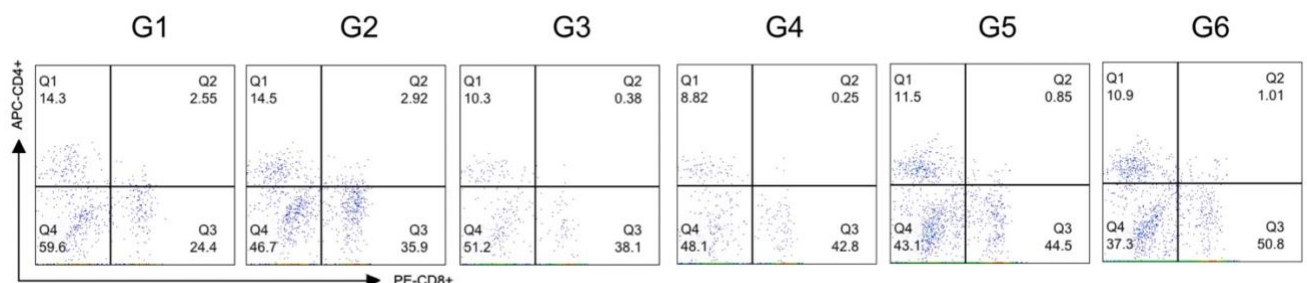


Fig. S16. Representative flow cytometry dot plot of CD8<sup>+</sup>T cell in the Tumor.  $n = 5$  mice

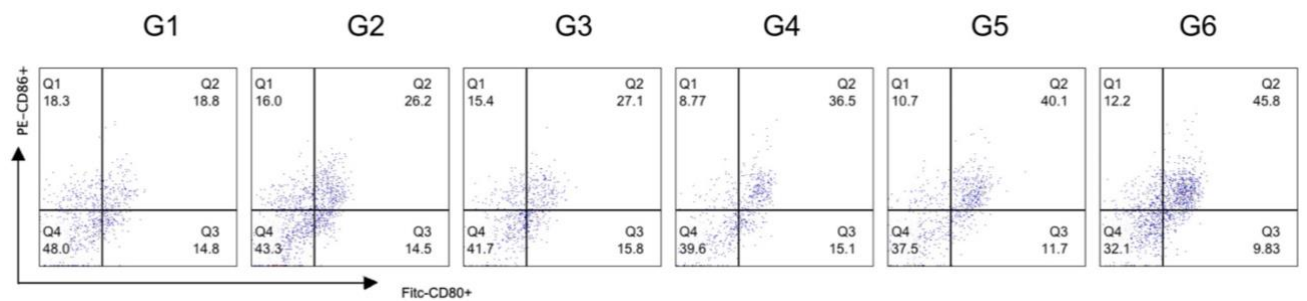


Fig. S17. Representative flow cytometry dot plot of mature DC cell in the Tumor.  $n = 5$  mice.

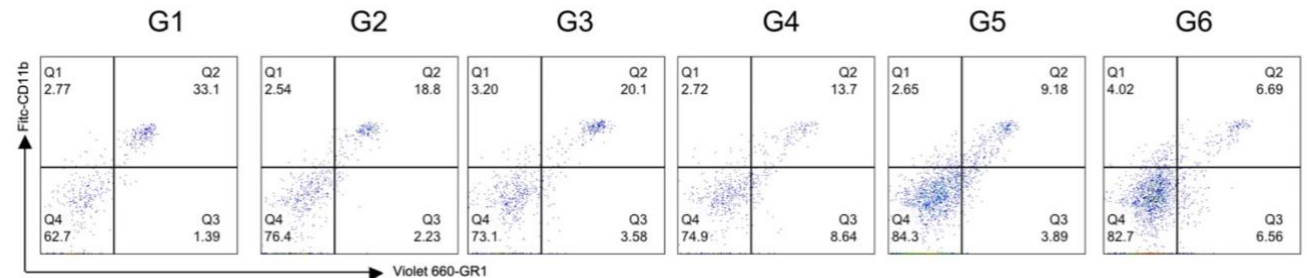


Fig. S18. Representative flow cytometry dot plot of MDSC cell in the Tumor.  $n = 5$  mice.

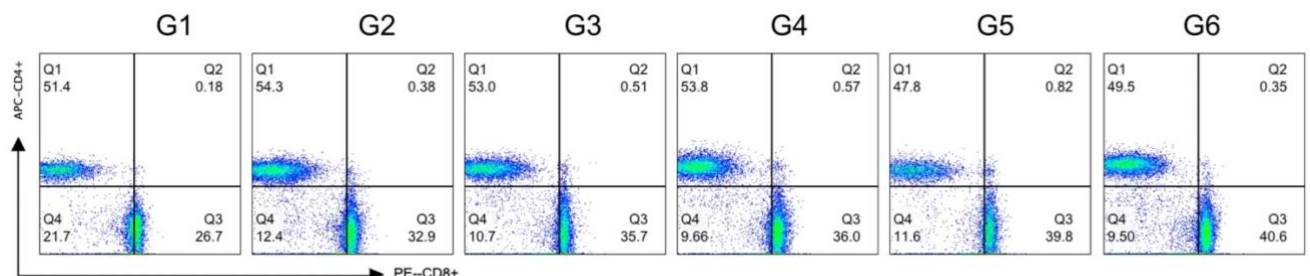


Fig. S19. Representative flow cytometry dot plot of CD8<sup>+</sup>T cell in the TDLN.  $n = 5$  mice.

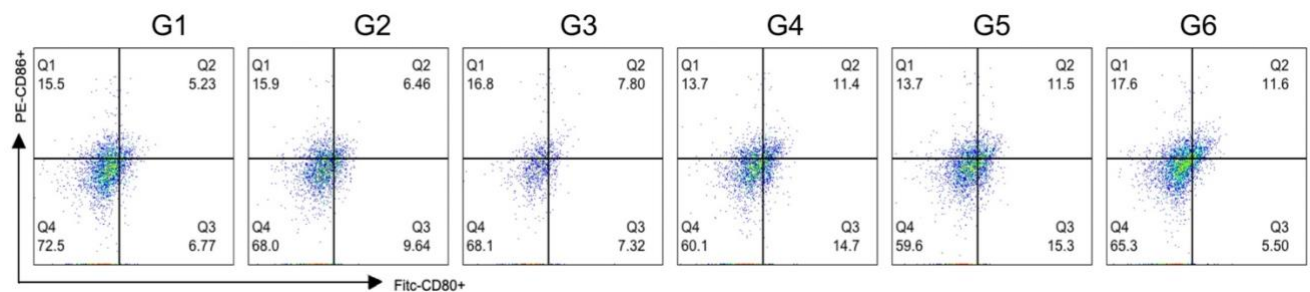


Fig. S20. Representative flow cytometry dot plot of mature DC cell in the TDLN.  $n = 5$  mice.

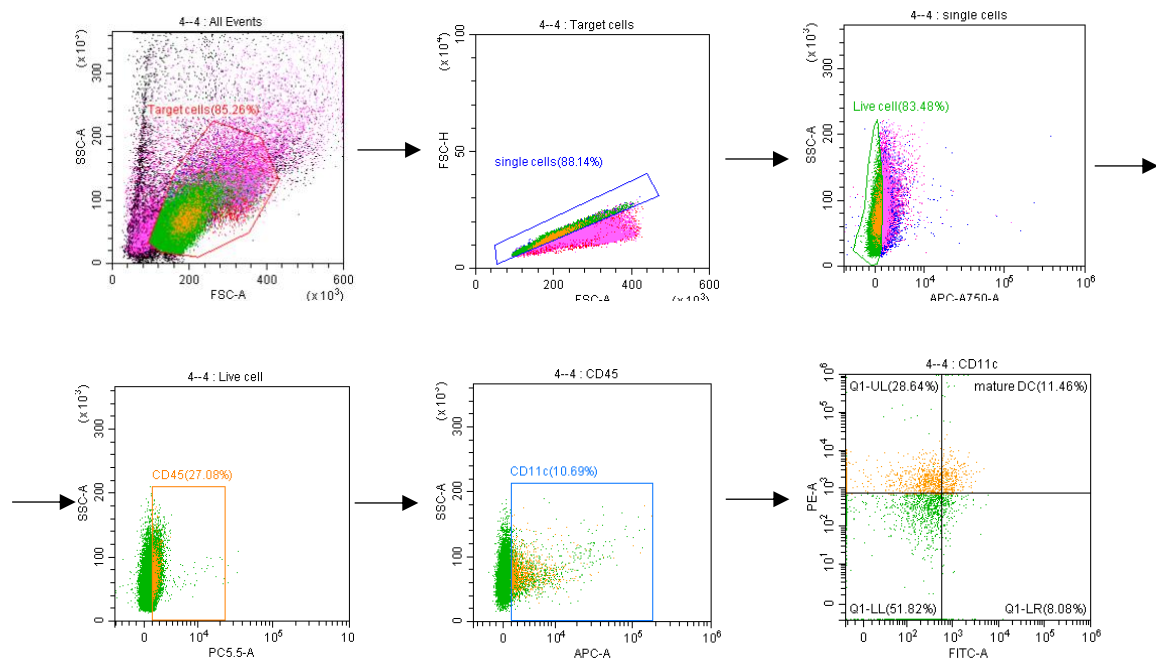


Fig. S21. Gating strategy to quantify mature DC cell in TDLN.

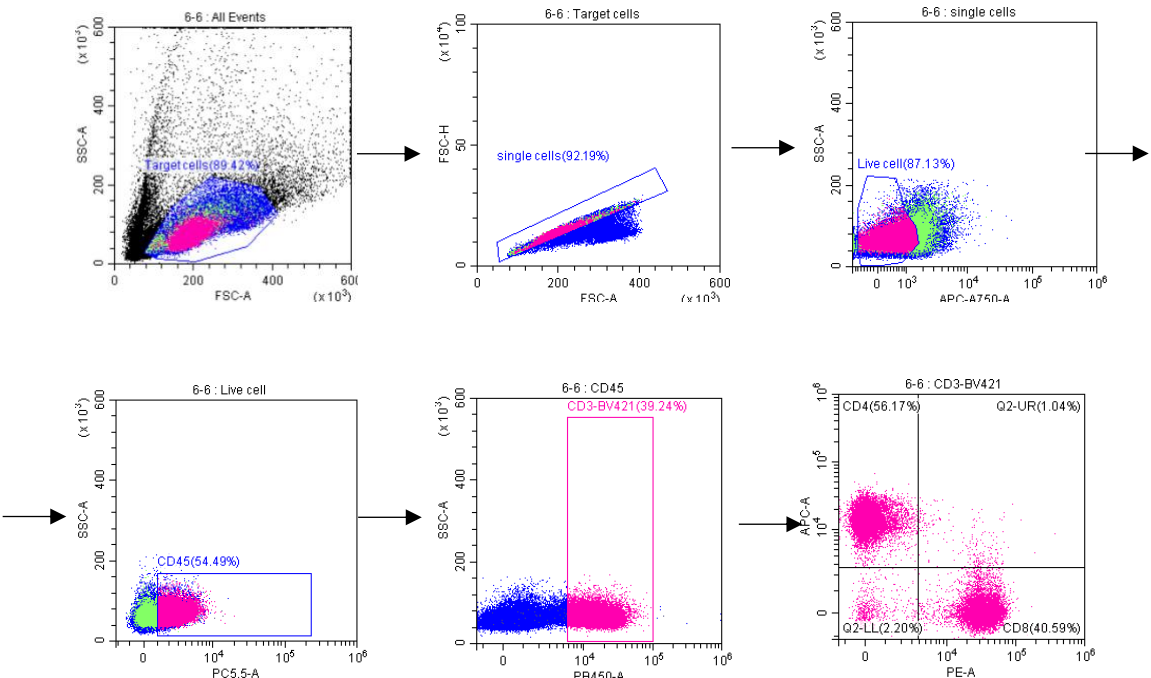


Fig. S22. Gating strategy to quantify CD8<sup>+</sup>T cell in TDLN.

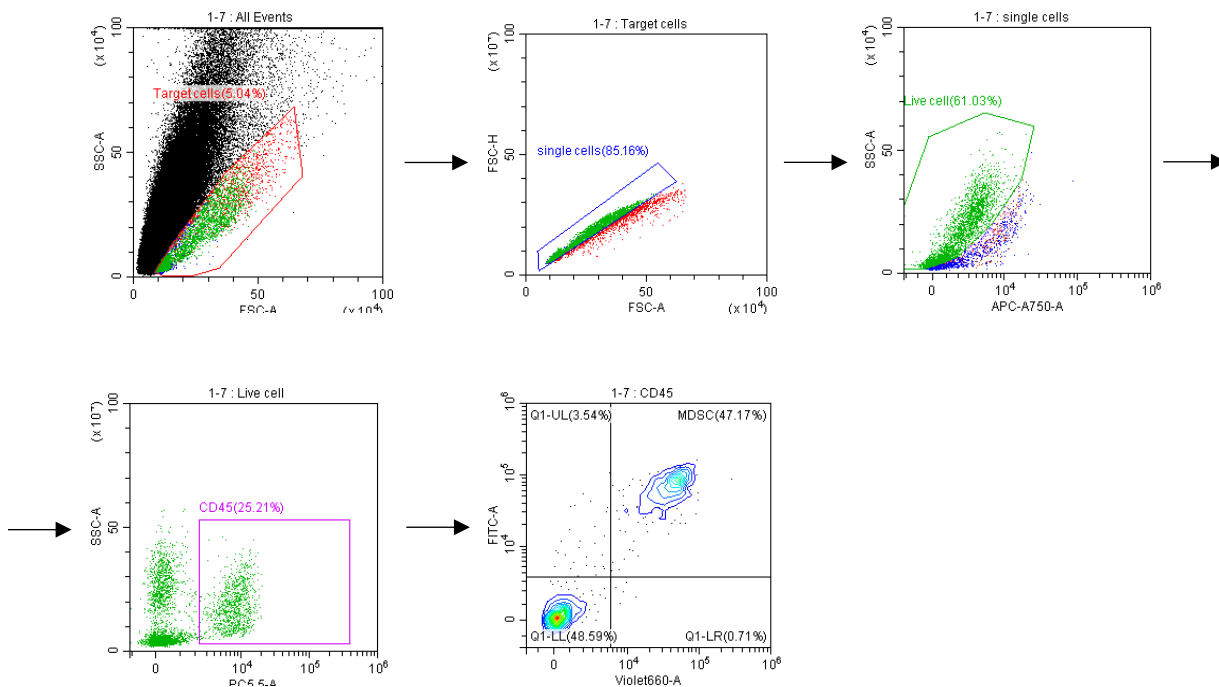


Fig. S23. Gating strategy to quantify MDSC cell in tumors.

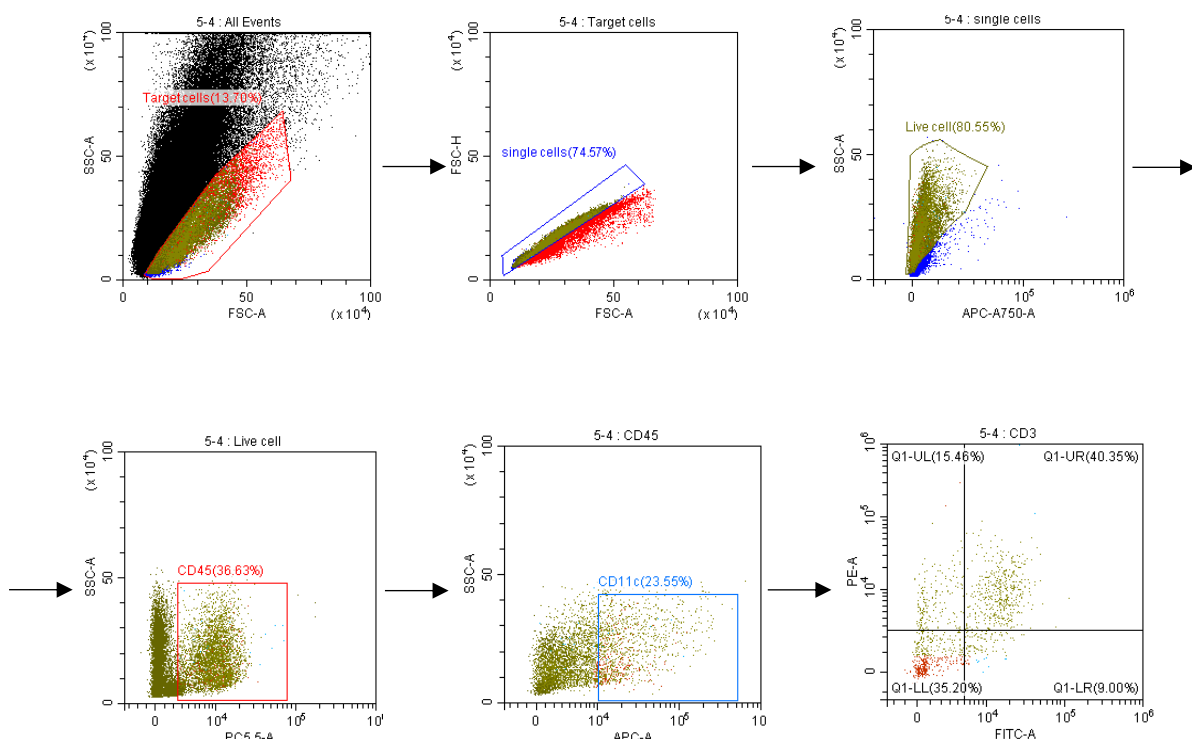


Fig. S24. Gating strategy to quantify mature DC cell in tumors.

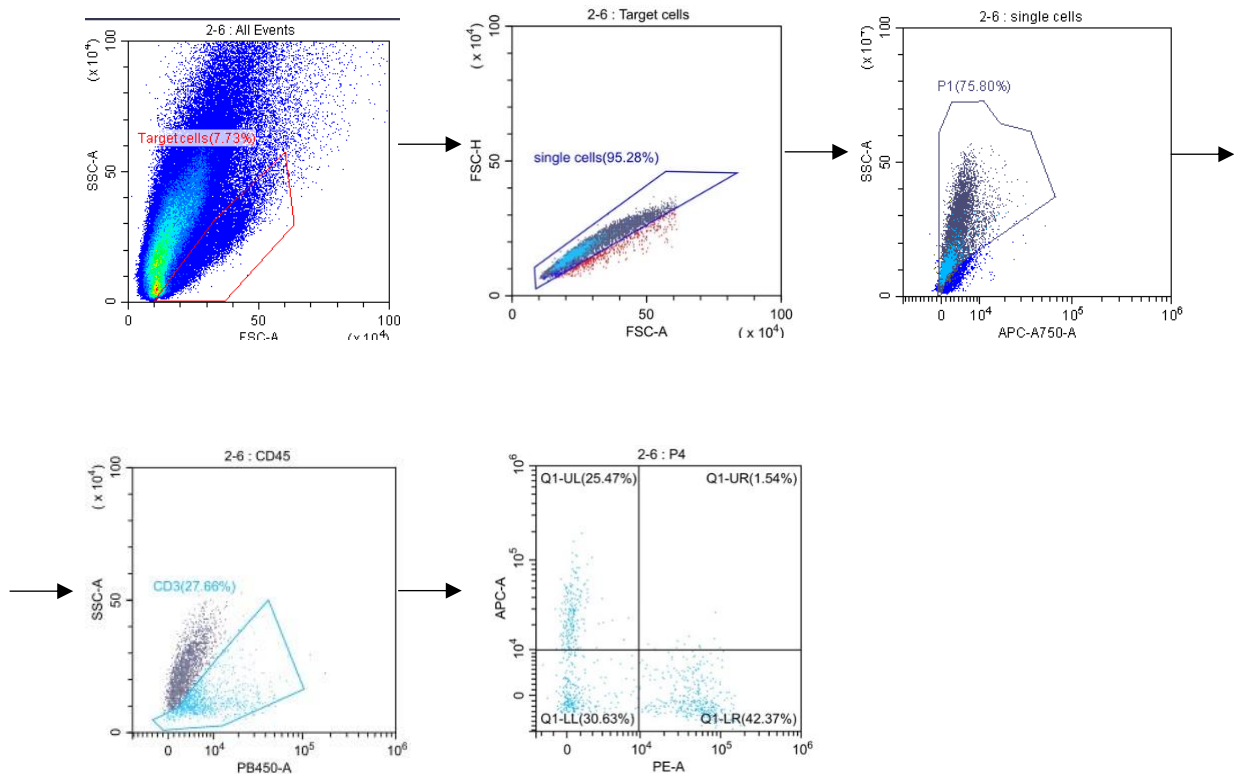


Fig. S25. Gating strategy to quantify CD8<sup>+</sup> T cell in tumors.